# Direct measurement of the n_TOF **NEAR** neutron fluence with **diamond detectors**

M. Diakaki[1], M. Bacak[2], C. Weiss[3,4], E. Griesmayer[3,4], C. Guerrero[5], E. Jericha[3], K. Kaperoni[1] ,
M. Kokkoris[1], A. Manna[6,7], N. Patronis[7], E. Stamati[2,7], R. Vlastou[1]
and the n_TOF Collaboration[8]

[1] National Technical University of Athens, Greece
[2] European Organization for Nuclear Research (CERN), Switzerland
[3] TU Wien, Atominstitut, Stadionallee 2, 1020 Wien, Austria
[4] www.cividec.at
[5] Universidad de Sevilla, Spain
[6] Istituto Nazionale di Fisica Nucleare, Sezione di Bologna, Italy
[7] Dipartimento di Fisica e Astronomia, Universit`a di Bologna, Italy
[8] University of Ioannina, Greece
[9] www.cern.ch/n_TOF

# The n_TOF NEAR station

- Very close to the Pb spallation target (~3m flight path)
- Commissioned in 2021

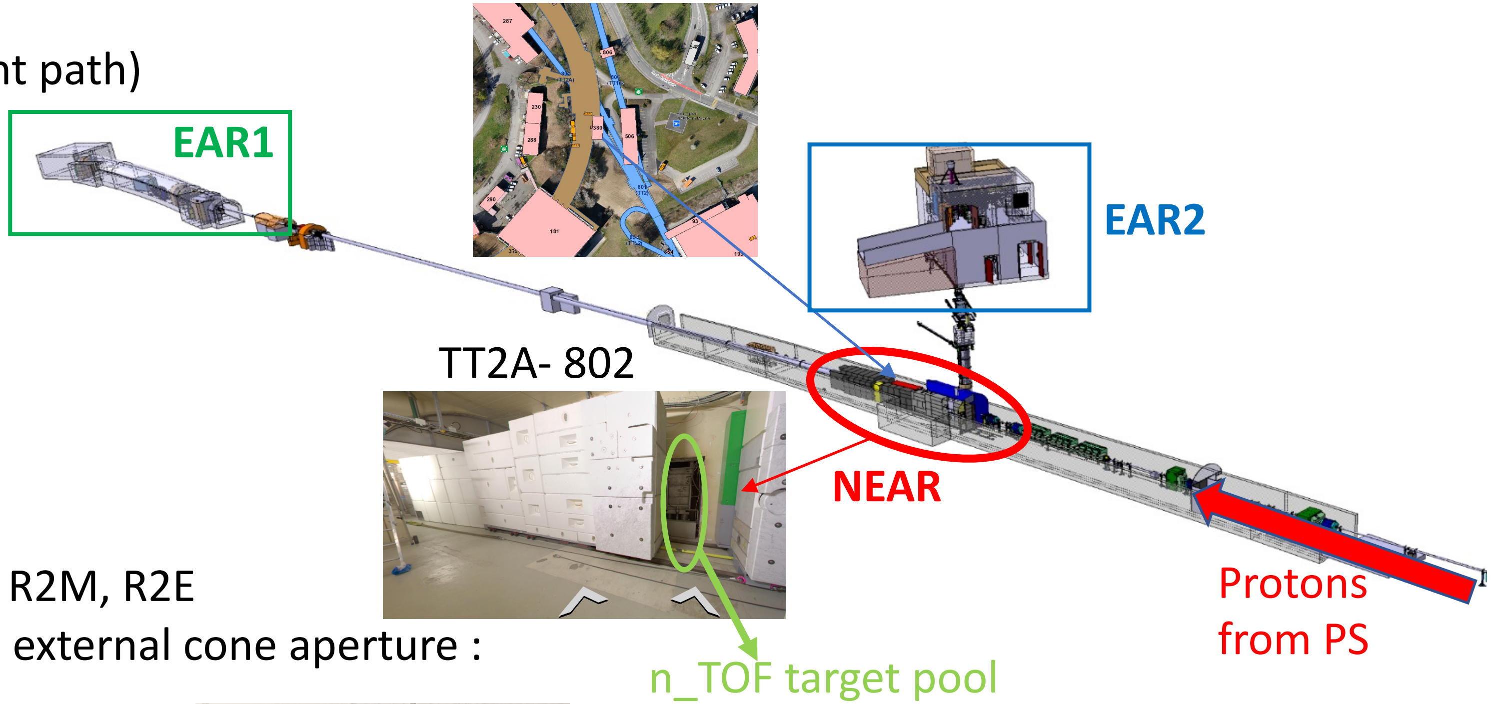


- n_TOF mixed field irradiation places for n_TOF, R2M, R2E

collaboration applications, along the center of the external cone aperture :

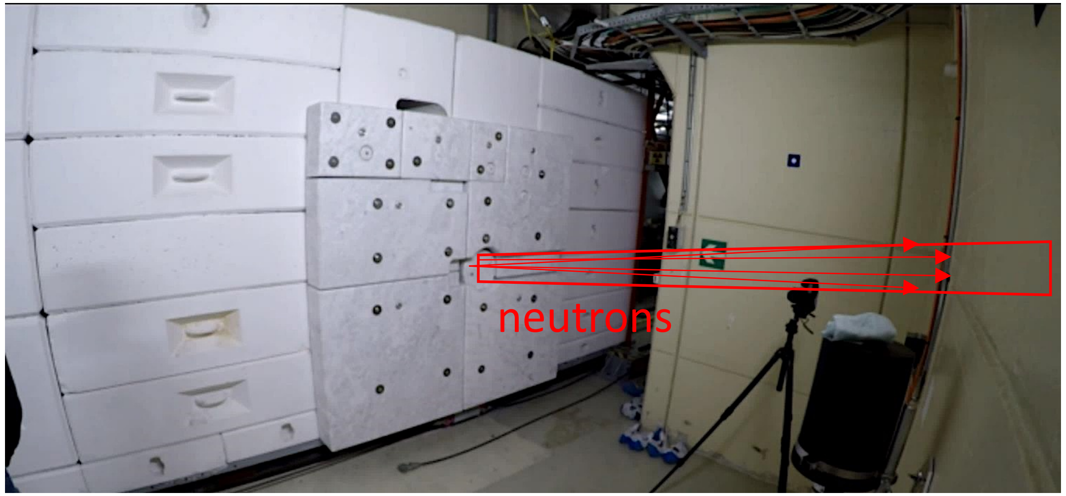


Possible applications :
- Nuclear Astrophysics
- Nuclear energy production studies
- Radiation damage studies
- ……

Photos from A.P. Bernardes presentation, n_TOF meeting 25/11/2021

# NEUTRON FLUENCE CHARACTERISATION at NEAR (simulations)

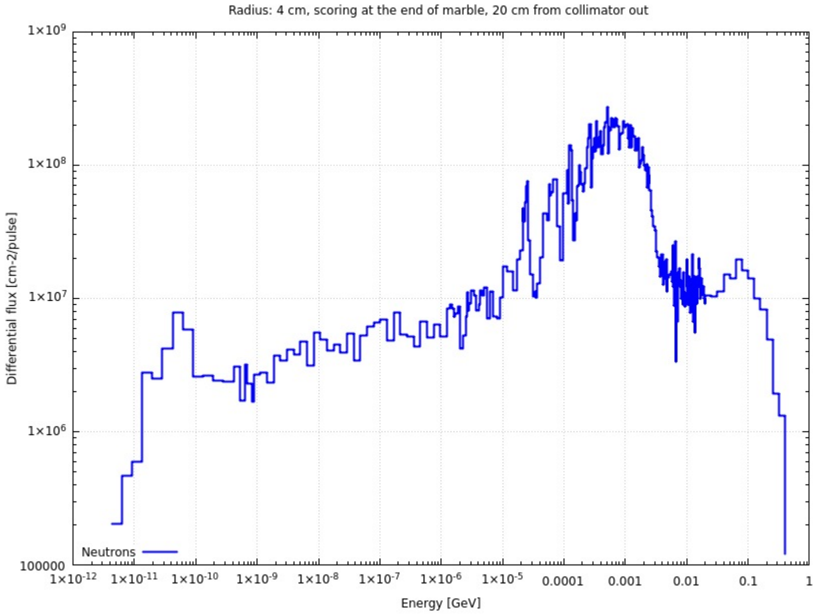


Radial dependence of neutron fluence:

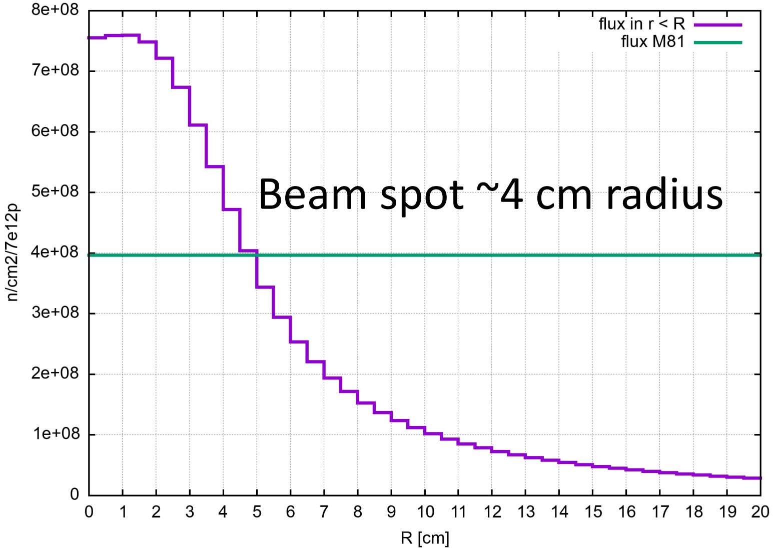


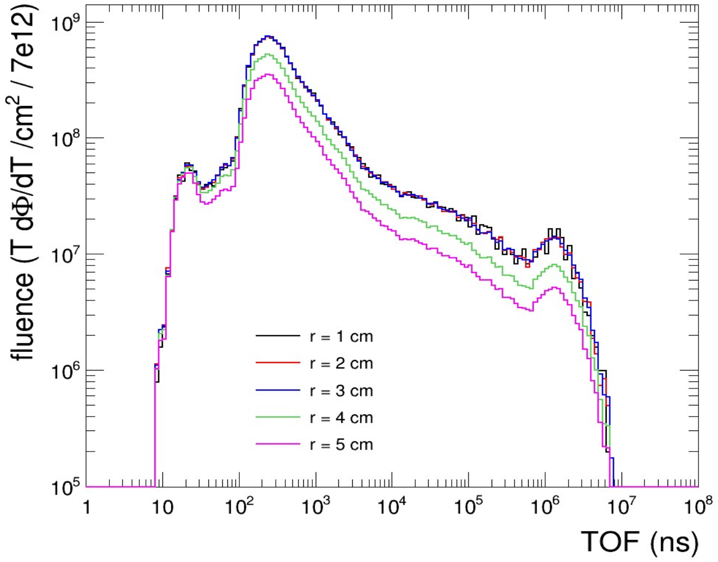

# NEUTRON FLUENCE CHARACTERISATION at NEAR (experimental)

To-date:

- Based on the **Multiple Foil Activation Analysis (MAM1** and **MAM2 configurations)** and the **Moderation-Absorption technique (ANTILOPE).**
- **Successful experimental campaigns in 2021, analysis ongoing.**

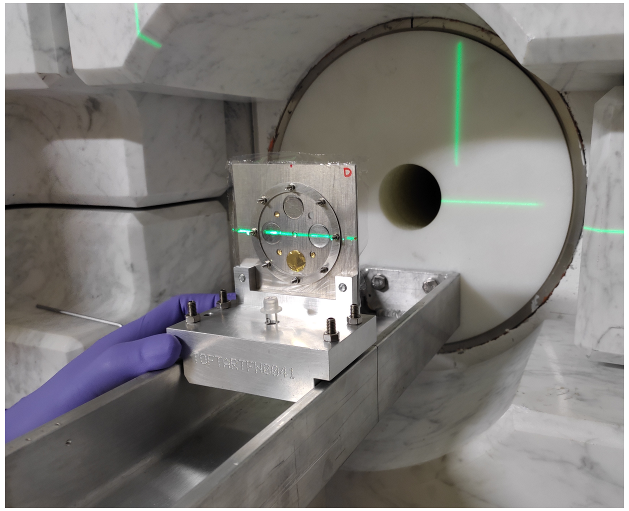

**MAM1**

**MAM2**


**ANTILOPE**

- The above mentioned techniques are based on neutron ACTIVATION, **no active detector yet at NEAR.**

With the present proposal we **aim to measure the neutron fluence at NEAR with an active detector, based on the diamond technology**. Detector development will be implemented in order to cope with the extremely high neutron fluence.

# Why diamond sensors??

- Diamond (allotrope of carbon) is characterised by
  - high radiation resistance,
  - high thermal conductivity /low thermal expansion coefficient
  - fast response time
  - high rigidity, biological and chemical inertia.
  - Good energy resolution (sub 1% for 5.5 MeV alpha particles)

Successfully used in
- neutron induced reaction studies
- neutron fluence measurements,

even in **harsh radiation environments** [1,2,3]

- Diamond sensor will be **especially developed by CIVIDEC Instrumentation [4]** for the flux measurement at NEAR:

Single crystalline sensor fabricated via the CVD (Chemical Vapour Deposition) technology.

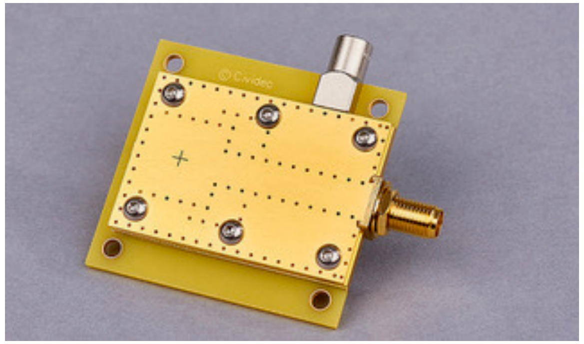

**Proposed characteristics**: 50 um thickness, 4x4 $mm^2$ active surface, $^6LiF$ converter

cividec Instrumentation

[1] E. Griesmayer et al., A novel neutron flux monitor at the Vienna TRIGA Mark II reactor, IAEA-CN-231-A.17, 2015
[2] M. Angelone and C. Verona, Review-Properties of Diamond-Based Neutron Detectors Operated in Harsh Environments, J. Nucl. Eng. 2021, 2, 422–470
[3] C. Cazzaniga et al., Characterization of the high-energy neutron beam of the PRISMA beamline using a diamond detector, 2016 JINST 11 P07012
[4] https://cividec.at/

# Neutron detection principle

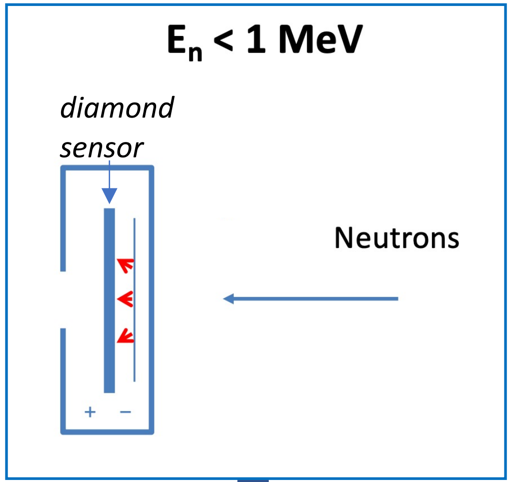


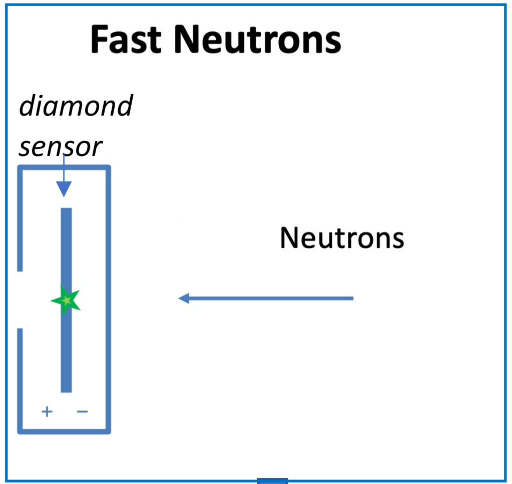


| Nuclear reaction | $E_{th}$ [MeV] | $Q$ [MeV] |
|---|---|---|
| $^{12}C(n,el)^{12}C$ | 0.0 | 0.0 |
| $^{12}C(n,\alpha)^{9}Be$ | 6.2 | -5.7 |
| $^{12}C(n,3\alpha)$ | 7.9 | -7.3 |
| $^{12}C(n,p)^{12}B$ | 13.6 | -12.6 |
| $^{12}C(n,d)^{11}B$ | 14.9 | -13.7 |
| $^{13}C(n,\alpha)^{10}Be$ | 4.1 | -3.8 |

based on a secondary reaction:
**$^{6}Li(n,t)^{4}He$**
Diamond sensor measures the secondary t and α particles

based on neutron interactions in the diamond:
**$^{12}C(n,el)$** and **$^{12}C(n,inl)$**
For $E_n$ > 6MeV also **$^{12,13}C(n,x\alpha/p)$**

*This principle already used in fission reactors and fusion tokamaks [1]*

- Schematics of proposed detector setup:

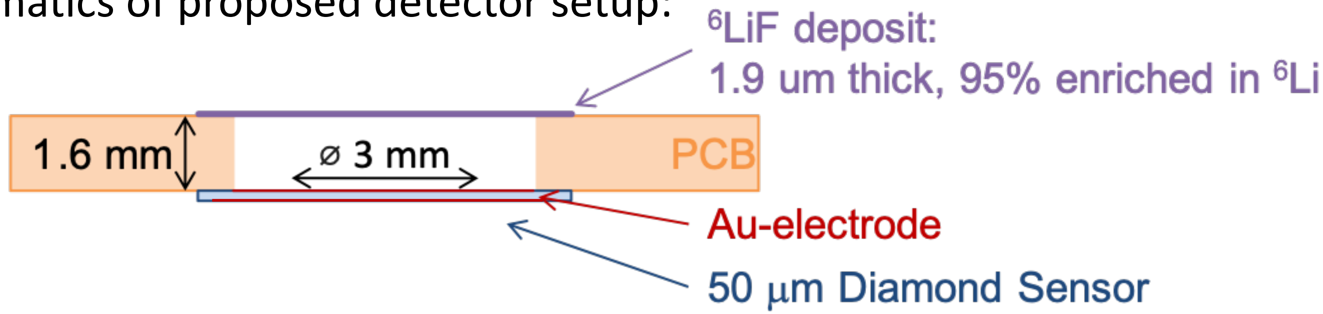


[1] M. Angelone and C. Verona, J. Nucl. Eng. 2021, 2, 422–470

# Estimated diamond det. response at NEAR (I)

**Expected Counting Rate estimation**, based on:

FLUKA simulations
of neutron flux
(scaled to detector area,
converted to neutron rate)

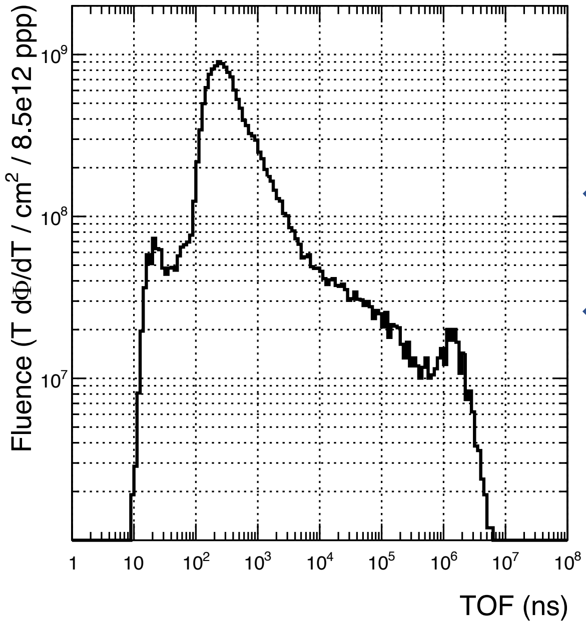


Neutron detection efficiency
vs neutron energy
(simulations)

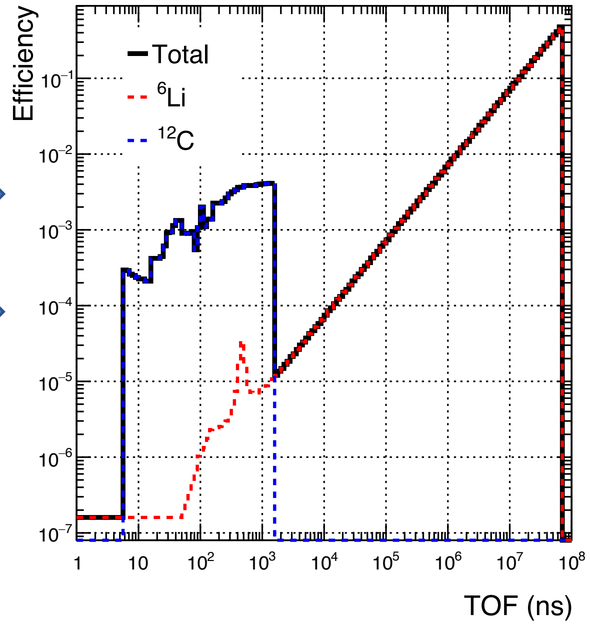


**Counting Rate:**

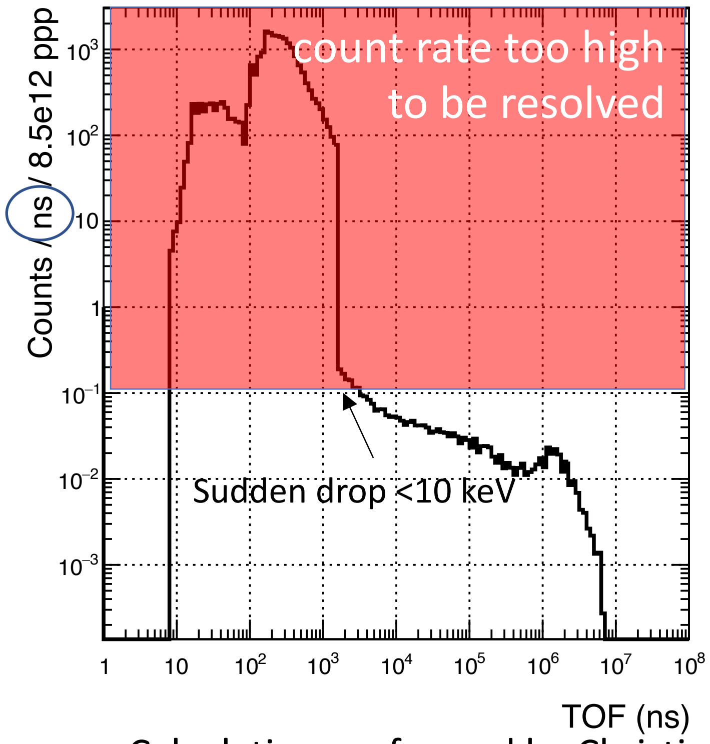


Calculation performed by Christina Weiss

- **Region of interest to astrophysics (<tens of keV) could be resolved.**
- **Detector current will be measured to extract the neutron fluence**

cividec Instrumentation

# Estimated diamond det. response at NEAR (II)

**Expected Detector current estimation**, based on:

FLUKA simulations
of neutron flux
(scaled to detector area,
converted to neutron rate)

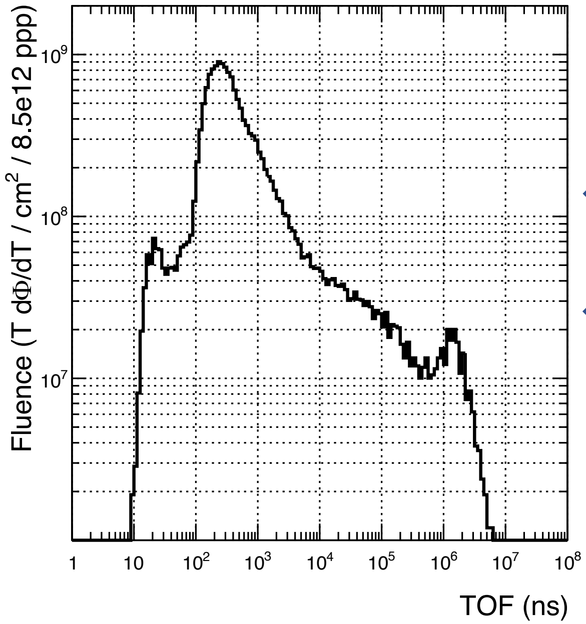


*Conversion Yield (Y)* *:

Y = $Q_m$ * ε

$Q_\mu$ = Mean charge / neutron interaction

ε = Neutron detection efficiency

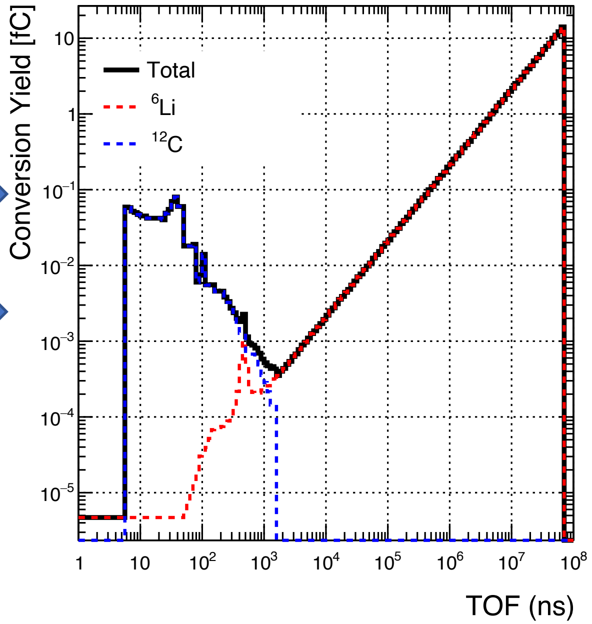


**Detector Current:**

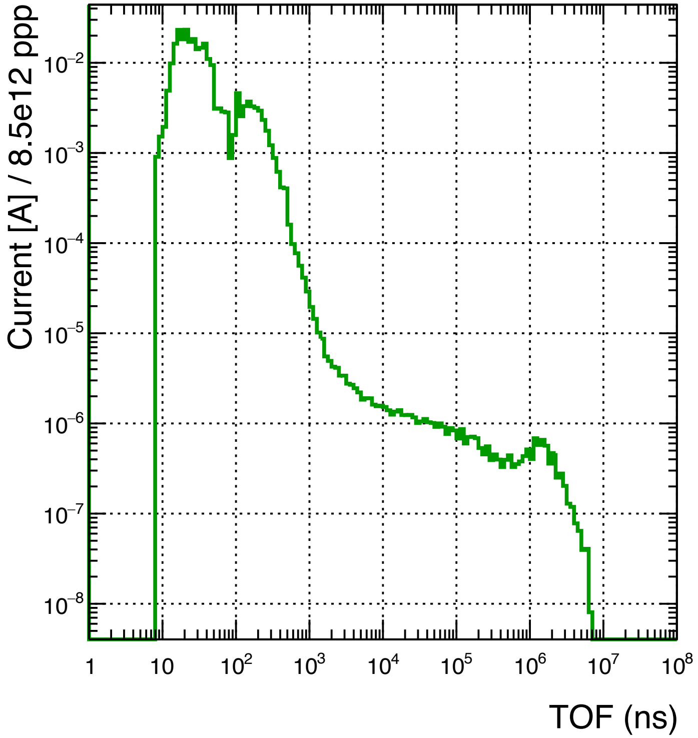


Calculation performed by Christina Weiss

***Extensive simulations and experimental validation:**

"Neutron spectroscopy with sCVD diamond detectors" , Pavel Kavrigin, PhD thesis, TU Wien, 2018.

cividec Instrumentation

# Estimated diamond det. response at NEAR (III)

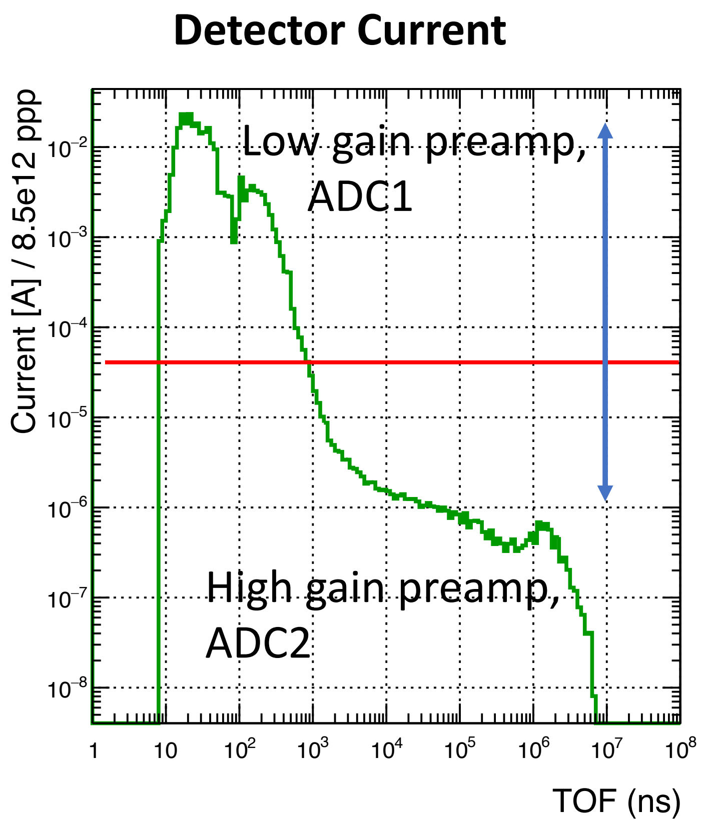


- Strong fluctuation of detector current (6 orders of magnitude)=> Detector current will be split and treated with 2 different amplifier gains + 2 ADC channels .
- Parallel readout in AC mode (Pulse Height mode). Development ongoing.

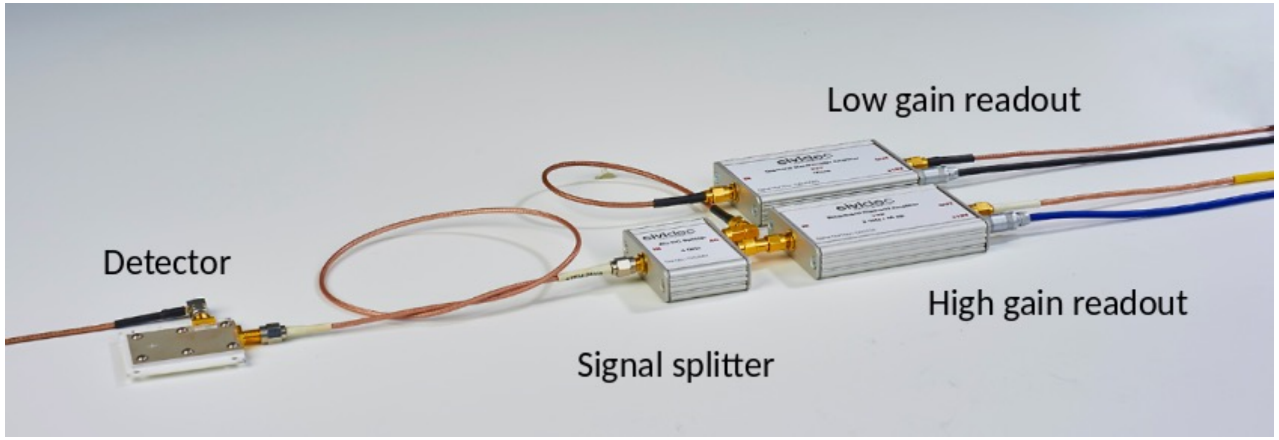


Storage of waveforms at 10-12 bit oscilloscopes for consequent offline analysis.

# Conclusion

- ***Neutron fluence measurement at NEAR with active detector for the first time, complementary to activation measurements.***
- ***Well proven detector technology (LHC, HiRadMat, CNGS, ChipIr, Tokamaks…), easy installation.***
- ***Upon successful completion, open the way to challenging in-beam measurements at NEAR.***

# BEAM TIME ESTIMATION

➢***EAR2: 3 × 10^17^** protons requested:*

Detector and electronics commissioning in well known beam (electronics adapted for EAR2)

➢***NEAR: 7 × 10^17^** protons requested:*

- $2 \times 10^{17}$ – debugging + intensity ramp
- $2 \times 10^{17}$ – **central position neutron fluence measurement**
- $1 \times 10^{17}$ – **beam homogeneity scan,** $10 \times 10$ $cm^2$ in 0.5 cm steps (detector mounted on special XY-table that can be moved remotely)
- $1 \times 10^{17}$ – **neutron fluence measurement** with $B_4C$ filter, useful for activation measurements [1]
- $1 \times 10^{17}$ – **neutron fluence measurement** without $^{6}Li$ converter, central position (elastic $^{12}C$ + delayed photons estimation…)

➢ In principle, parallel to measurements in EAR1 and EAR2.

**Thank you!**

[1] E. Stamati et al., CERN-INTC-2022-008; INTC-P-623 (2022)

# Extra slides

# Estimated diamond det. response at NEAR (IV)

- Very low intensity pulses (5e10 ppp):

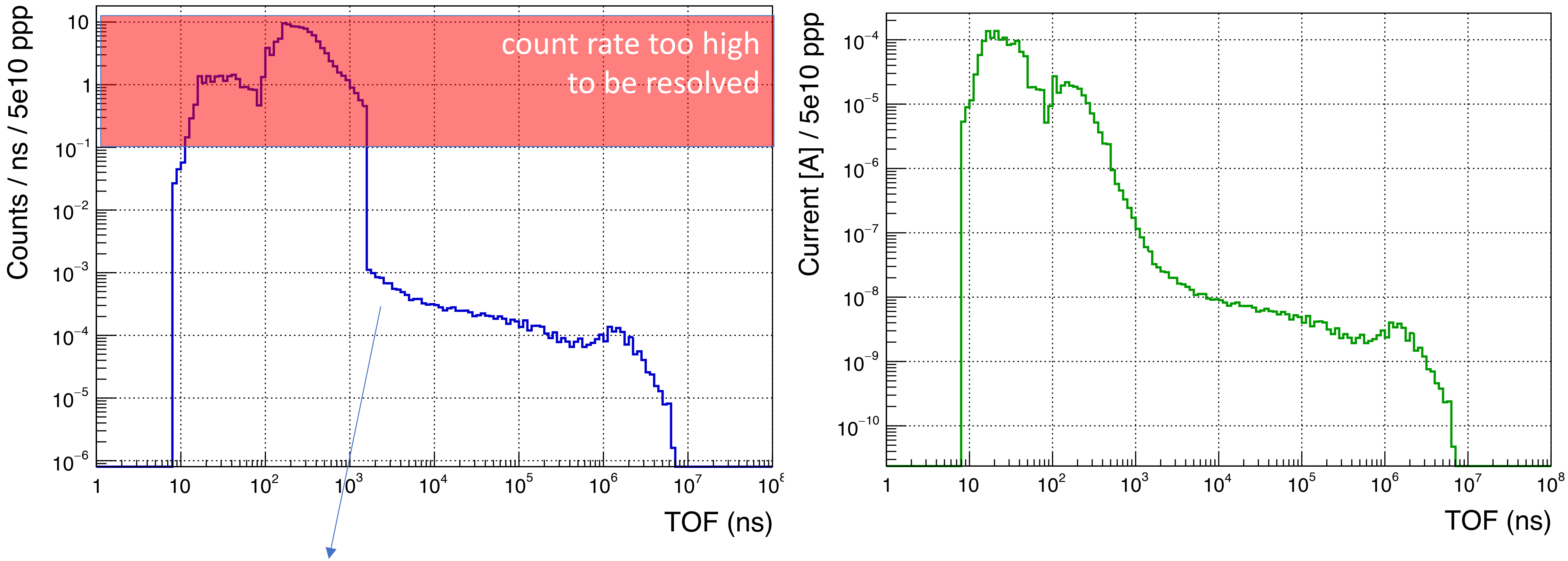


Measurement of the AC detector signal will be possible

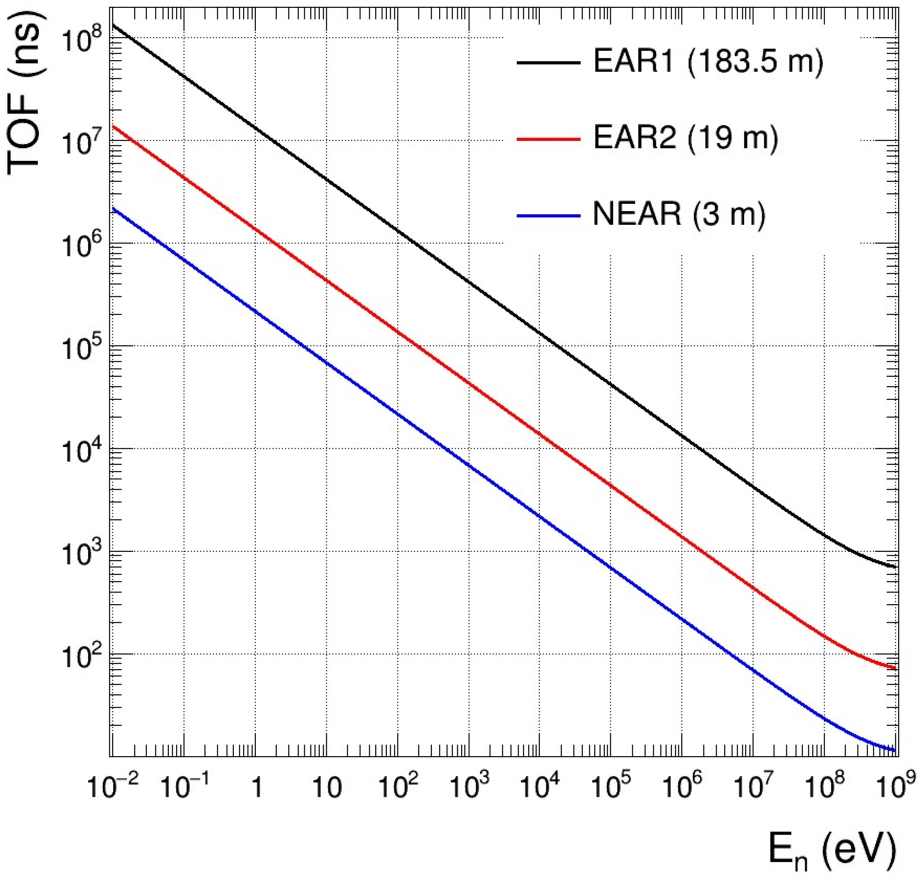
TOF (ns)
EAR1 (183.5 m)
EAR2 (19 m)
NEAR (3 m)
$E_n$ (eV)

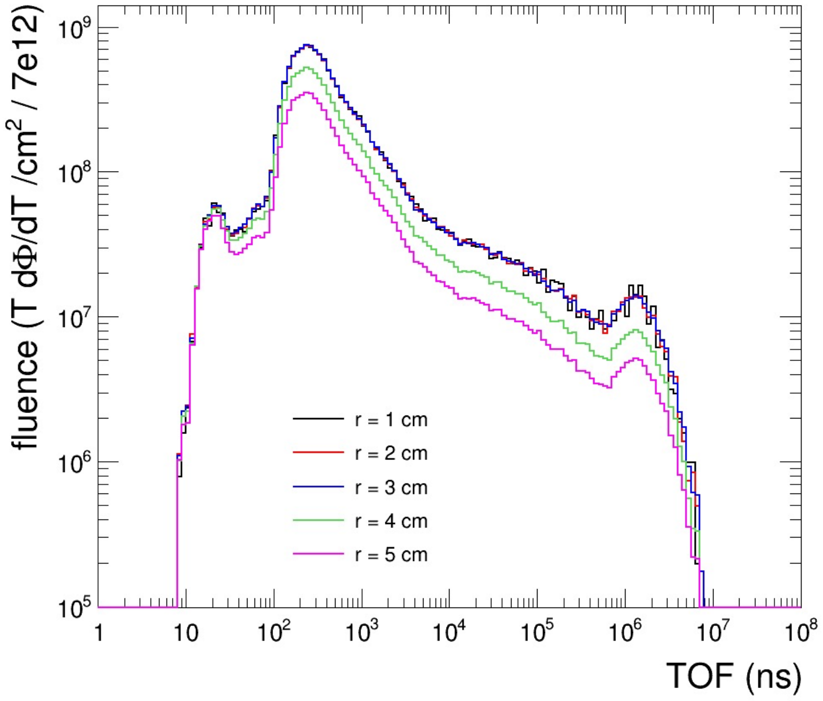
fluence (T dΦ/dT /cm$^2$ / 7e12)
r = 1 cm
r = 2 cm
r = 3 cm
r = 4 cm
r = 5 cm
TOF (ns)

# Conversion yield

| Energy Interval | ε (ENDF/B-VIII.0) | $Q_{\mu}$ [fC] |
|---|---|---|
| $E_n$ < 10 keV | $^{6}Li(n,a)t$ | Q-value/2/$E_{ion}$*$q_{el}$ = 29.4 fC |
| 10 keV < $E_n$ < 1 MeV | $^{6}Li(n,a)t$<br>$^{12}C(n,tot)$ | Q-value/2/$E_{ion}$*$q_{el}$ = 29.4 fC<br>$f_1$( $E_n$ ), see below |
| $E_n$ > 1 MeV | $^{12}C(n,tot)$ | $f_2$( $E_n$ ), Geant4 P. Kavrigin |

ionisation energy of diamond

elementary charge

$$f_1(E_n) = E_n * 0.286 / E_{ion} * q_{el} * 0.5$$

$E_{max}$ for $^{12}C$ nucleus in $^{12}C(n,el)$

assuming isotropic scattering, we measure on average ½ of the total charge

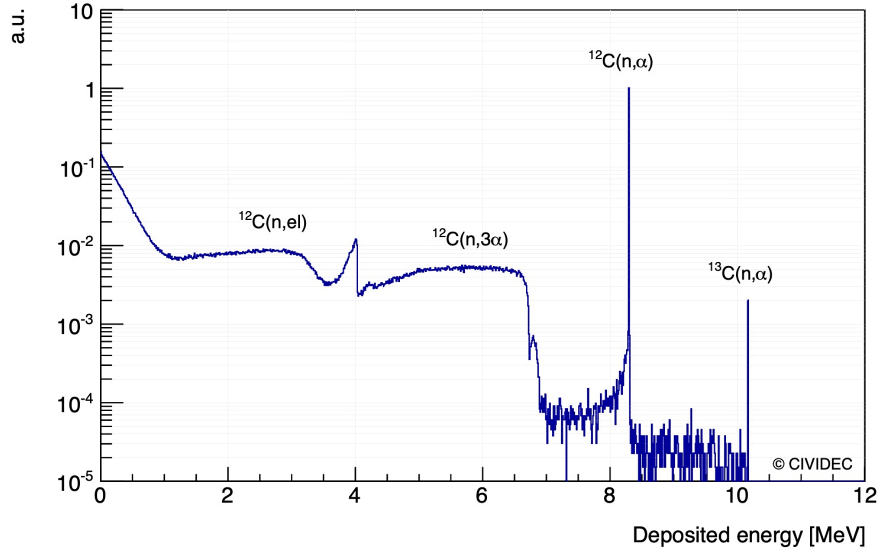


Figure 3.23: Deposited energy spectrum of 14 MeV neutrons in 500 $\mu$m diamond.

**Table 1.** Diamond parameters [1].

| Parameter | Value |
|---|---|
| Atomic Number | 6 |
| $E_g$ at 300 K (eV) | 5.470 |
| Density (g·cm$^{-3}$) | 3.515 |
| $\varepsilon_p$ (eV) | 13 |
| Fusion temperature (°C) | 4100 |
| Electron mobility (cm$^2$V$^{-1}$s$^{-1}$) at 300 K | 1800–2200 |
| Hole mobility (cm$^2$V$^{-1}$s$^{-1}$) at 300 K | 1200–1600 |
| Breakdown voltage (Vcm$^{-1}$) | >$10^7$ |
| Thermal conductivity $\sigma_T$ (Wcm$^{-1}$K$^{-1}$) | 20 |
| Saturation velocity $v_{sat}$ (cm s$^{-1}$) | $2.7 \times 10^7$ |
| Resistivity $\rho$ (ohm cm) | >$10^{13}$ |
| Intrinsic carrier density at 300 K (cm$^{-3}$) | <$10^3$ |
| Dielectric constant | 5.7 |
| Energy to displace an atom (eV) [1] | 37.5–47.6 |

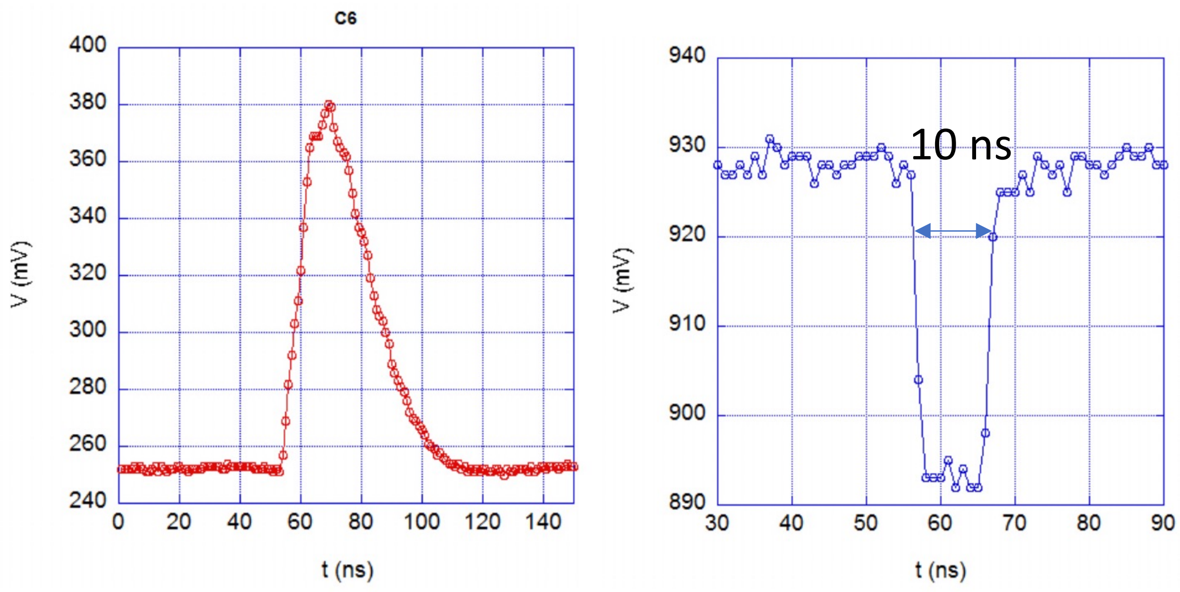


**Figure 1**. Alpha particle signals recorded with a SDD using CIVIDEC C6 (on the left) and C2 (on the right) preamplifiers.

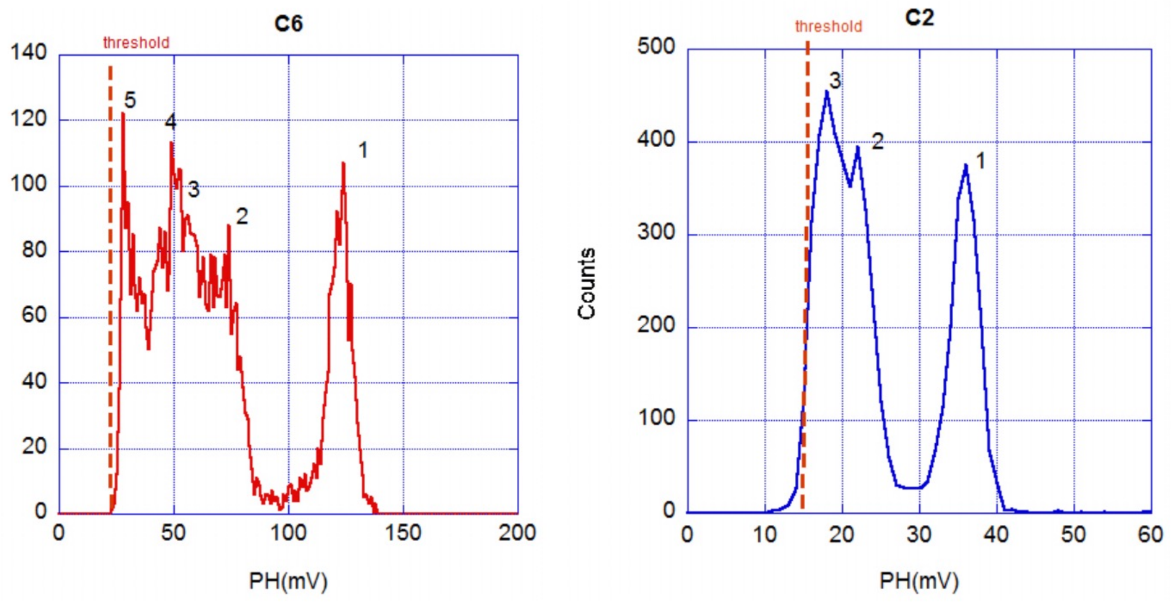


**Figure 2**. Pulse Height Spectra of an alpha source of Ra-226 recorded with a SDD using CIVIDEC C6 (on the left) and C2 (on the right) preamplifiers. Numbers from 1 to 5 tag the peaks as in table 1. A dashed vertical line indicates the acquisition threshold.

From Cazzaniga et al., 2016 JINST 11 P07012

# Gamma background, grossier estimation from EAR2 simulations

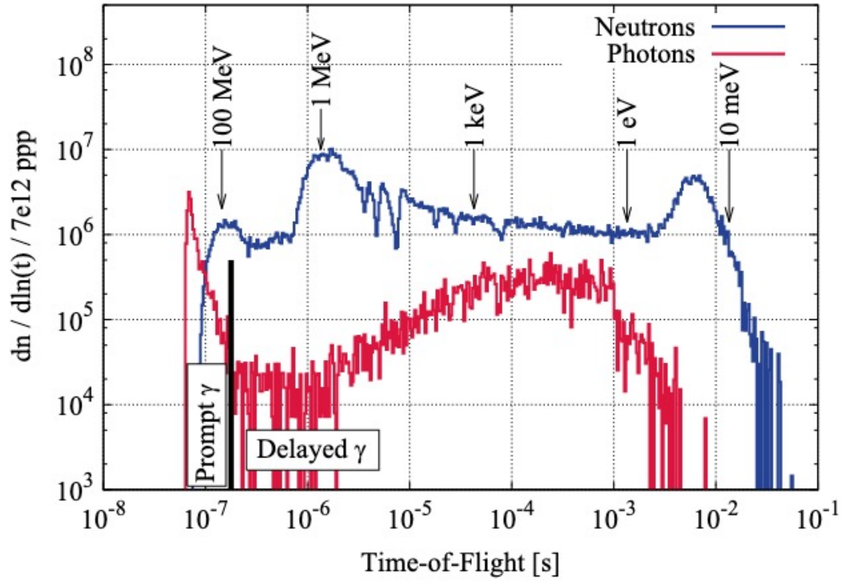


In Figure 3.17 the conversion yield of the $\gamma$ interaction in diamond is shown.

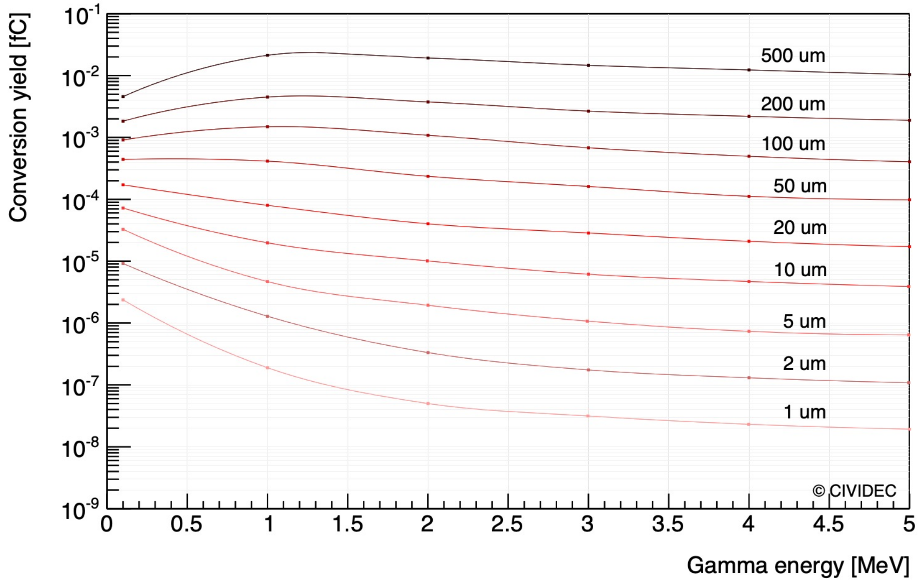


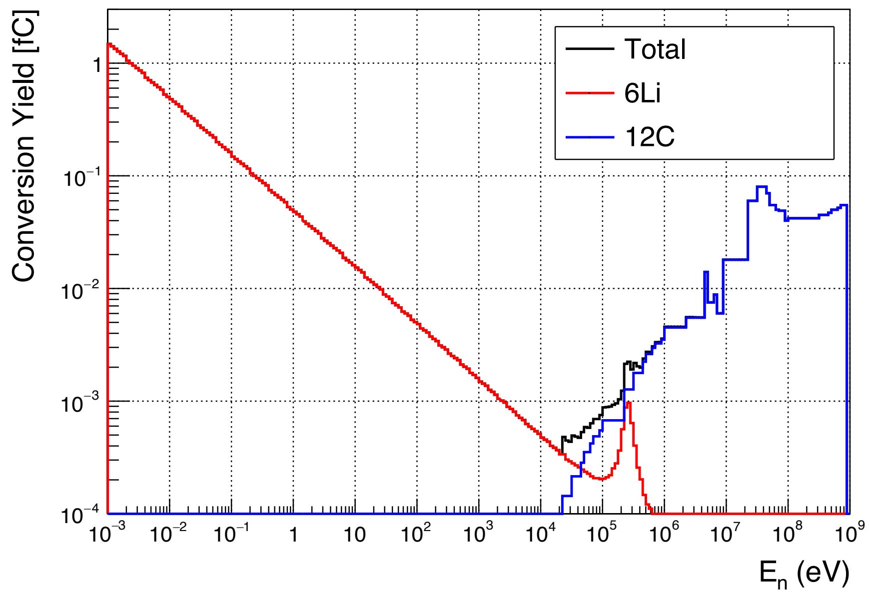


Delayed gammas not expected to significantly influence the measurement

## Resolution for TOF measurements at NEAR

# NEAR

Flight_path assumed: 4m

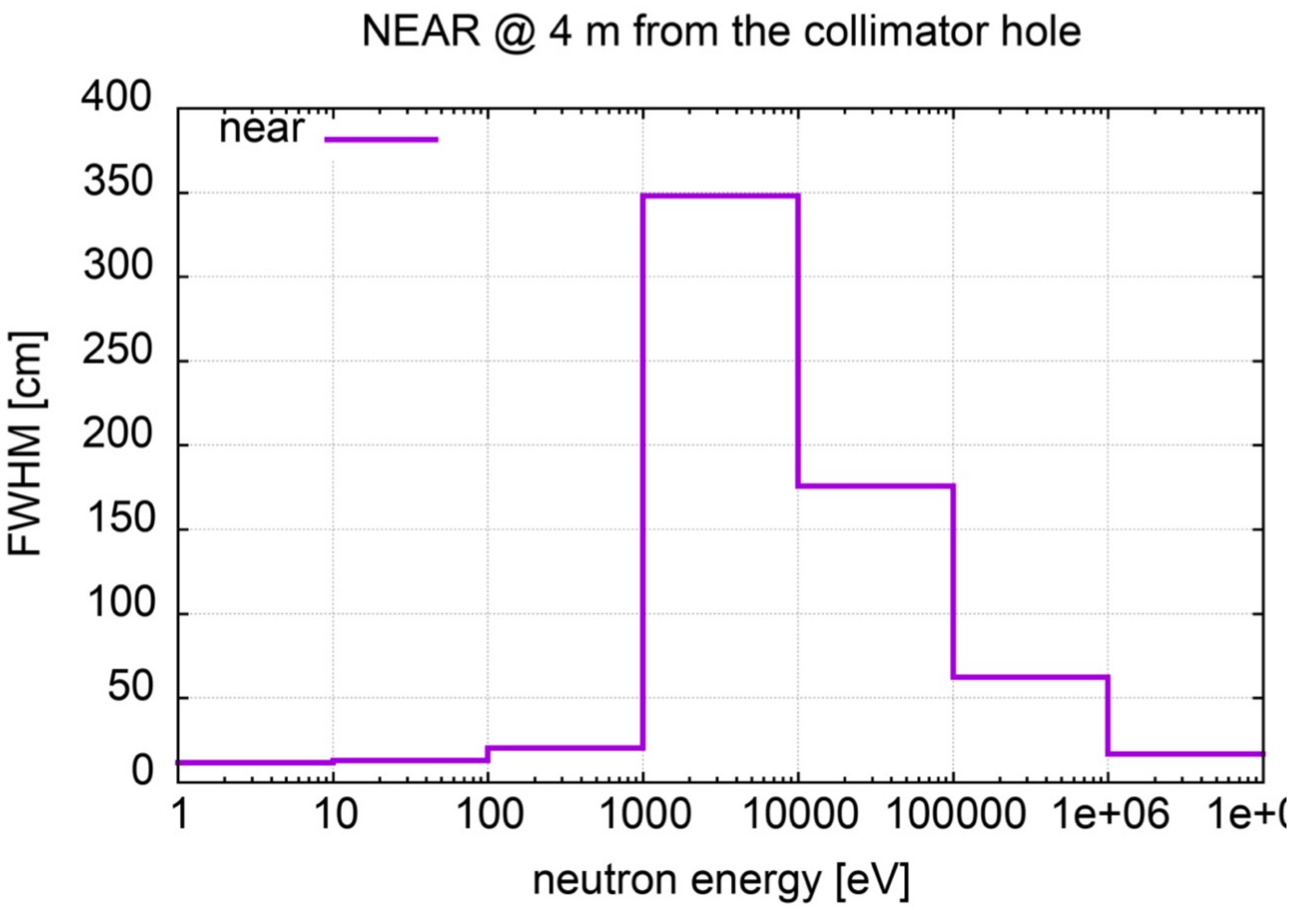


#area : data/NEAR_score
#flight-path [cm] : 400.0

| # energy range [eV] | | FWHM [cm] | FWTM [cm] | dE/E |
|---|---|---|---|---|
| 1.0 | 10.0 | 11.7 | 39.0 | 5.8e-02 |
| 10.0 | 100.0 | 13.0 | 45.7 | 6.5e-02 |
| 100.0 | 1000.0 | 20.2 | 197.6 | 1.0e-01 |
| 1000.0 | 10000.0 | 390.6 | 577.5 | 2.0e+00 |
| 10000.0 | 100000.0 | 175.8 | 483.5 | 8.8e-01 |
| 100000.0 | 1000000.0 | 62.4 | 157.8 | 3.1e-01 |
| 1000000.0 | 10000000.0 | 16.6 | 48.3 | 8.3e-02 |

#area : data/EAR2_scorewin
#flight-path [cm] : 2000.0

| # energy range [eV] | | FWHM [cm] | FWTM [cm] | dE/E |
|---|---|---|---|---|
| 0.1 | 1.0 | 3.5 | 15.3 | 3.5e-03 |
| 1.0 | 10.0 | 3.9 | 9.2 | 3.9e-03 |
| 10.0 | 100.0 | 4.2 | 11.3 | 4.2e-03 |
| 100.0 | 1000.0 | 5.4 | 15.9 | 5.4e-03 |
| 1000.0 | 10000.0 | 10.1 | 31.9 | 1.0e-02 |
| 10000.0 | 100000.0 | 24.3 | 87.8 | 2.4e-02 |
| 100000.0 | 1000000.0 | 63.4 | 154.7 | 6.3e-02 |
| 1000000.0 | 10000000.0 | 27.2 | 74.7 | 2.7e-02 |

From the presentation of A. Mengoni, n_TOF collaboration meeting, 30-31 May 2022

# MACS AT NEAR

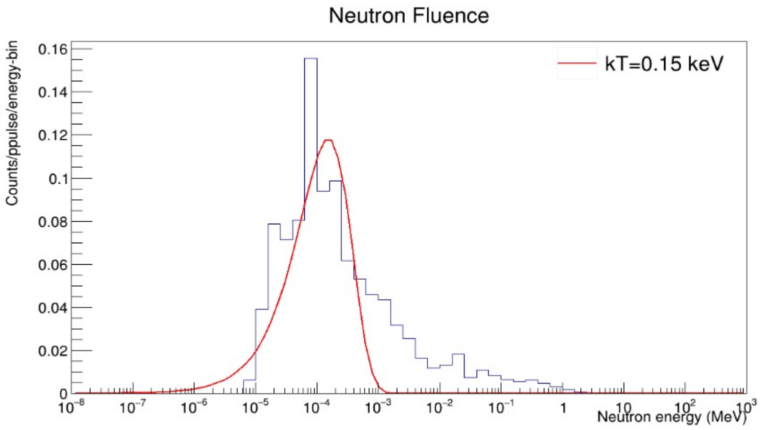


Figure 3: *Neutron energy distribution obtained at the irradiation point, using a 5 mm thickness B4C cylinder and comparison with a Maxwell-Boltzmann distribution with most probable thermal energy kT =*

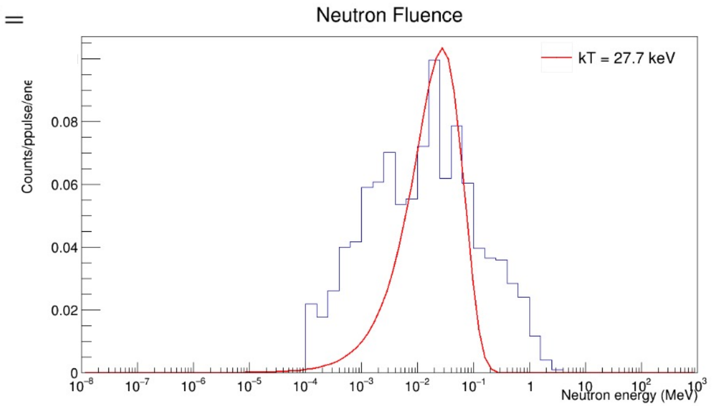


Figure *4: Neutron energy distribution obtained at the irradiation point, using a* 20 mm *thickness B4C cylinder and comparison with a Maxwell-Boltzmann distribution with most probable thermal energy kT = 27.7 keV.*

[1] E. Stamati et al., CERN-INTC-2022-008; INTC-P-623 (2022)